Journal of Applied Polymer Science

# Grafting of Acrylic Acid-*co*-Itaconic Acid onto ePTFE and Characterization of Water Uptake by the Graft Copolymers

**Norsyahidah Mohd Hidzir,[1] Qianhui Lee,[2] David J. T. Hill,[1] Firas Rasoul,[2] Lisbeth Grøndahl[1]**
[1]School of Chemistry and Molecular Biosciences, University of Queensland, Brisbane, Queensland 4072, Australia
[2]Australian Institute of Bioengineering and Nanotechnology, University of Queensland, Brisbane, Queensland 4072, Australia
Correspondence to: L. Grøndahl (E-mail: l.grondahl@uq.edu.au)

**ABSTRACT:** Expanded polytetrafluoroethylene, ePTFE, is an attractive material for use as the implant in facial reconstruction surgery because it is bioinert; however, its low surface energy does not facilitate a strong interfacial bond with bone and thus for some applications the surfaces need to be modified to enhance their bone-integration properties. The surface modification of ePTFE membranes with copolymers of acrylic acid (AA) and itaconic acid (IA) using *in situ* gamma radiation induced grafting has been studied. Solutions with AA mole fractions ranging from 0.4 to 1.0 have been investigated. Graft yields of 35–50% with water uptakes of greater than 300% were obtained using 3 mol $L^{-1}$ aqueous solutions of the monomers and a total incident dose of 10 kGy. The grafts were characterized by Fourier transform infrared and X-ray photoelectron spectroscopy analyses and the compositional microstructure of the grafted copolymers was investigated. The water uptake by the grafted membranes displayed a complex dependence on polymer chemistry and topology. © 2014 Wiley Periodicals, Inc. J. Appl. Polym. Sci. **2015**, *132*, 41482.

**KEYWORDS:** biomedical applications; grafting; membranes; radical polymerization; swelling

Received 27 July 2014; accepted 9 September 2014
**DOI: 10.1002/app.41482**

## INTRODUCTION

Polymers have been widely used as biomaterials for more than half a century, and polytetrafluoroethylene, PTFE, because of its bio-stability has found many applications as a biomaterial, ranging from abdominal wall reconstruction to vascular grafts.[1,2] In many of these applications so-called expanded PTFE, ePTFE, is the material of choice because of its improved flexibility and porosity resulting from its node-fibril morphology.[3] To form ePTFE, PTFE is stretched at a temperature above its first crystalline melting point, which leads to the formation of a fibrillar structure and associated micron-sized pores in the polymer matrix.[3] This open network structure allows ePTFE to be much more pliable as a membrane than PTFE and also changes other physical properties of the material. However, while ePTFE is an ideal biomaterial in many respects, its inherent chemical inertness serves as a disadvantage to its integration with some body tissues, such as bone. Thus, for applications of ePTFE such as tissue space fillers in facial reconstruction, it is desirable to modify its low surface energy by surface grafting a polar monomer onto the surface so as to improve tissue integration.[2] Ionic groups (i.e., phosphate and carboxylate) have been shown to enhance mineralization *in vitro* and thus bone-bonding ability.[2]

A wide variety of monomers have been used in modifying the surface of PTFE or ePTFE, including 2-(methacryloyloxy)ethyl phosphate,[4] 2-hydroxyethyl methacrylate,[5] and acrylic acid (AA).[6–12] The grafting of vinyl monomers onto the PTFE surface requires the formation of radicals at the surface of the polymer to initiate polymerization, and thus form a strong chemical bond between the ePTFE and the grafted polymer. However, because of the high strength of the carbon-fluorine bond, high energy radiolysis using $\gamma$, electron beam or plasma radiations are the methods of choice for initiating these grafting reactions.[13] Specifically, for grafting of AA onto ePTFE, a number of these methods have been explored including pre-irradiation grafting using gamma rays,[6] simultaneous grafting using gamma rays,[7] He,[8,9] Ar,[10] or $O_2$ plasma,[11] as well as $CO_2$ microwave plasma induced grafting.[12]

It has long been recognized that copolymers of AA and itaconic acid (IA), (e.g., P(AA-*co*-IA)) provide better properties than poly(acrylic acid) (PAA) alone in forming the matrices of glass ionomers used for dental applications.[14] In these applications, it is fundamentally important for the glass ionomers to bond strongly with the surrounding dental tissues, which include hydroxyapatite. It has been proposed[15,16] that the incorporation of a low concentration of IA, typically 10–20%, disrupts the regular structure of the PAA homopolymer. This disruption allows improved bonding of the copolymer with the $Ca^{2+}$ of hydroxyapatite, while maintaining a high solubility of the matrix

copolymer in water. P(AA-*co*-IA) has also been patented for use in removing the calcium deposits found in boiler scale[17] or for use as an antiscalant in prevention of formation of $Ca^{2+}$ deposits such as those which can be formed, for example, during sea water evaporative desalination.[18]

There have been only a few reports of the formation and properties of P(AA-*co*-IA) hydrogels,[19–21] but, to the best of our knowledge, there have been no previous reports of the surface grafting of AA-*co*-IA on to ePTFE. However, there have been some reports of AA-*co*-IA grafting onto other carbon-based polymers, including grafting on carboxymethyl cellulose,[22] collagen,[23,24] or cotton.[25] In these studies, the grafting was chemically initiated and the variables such as comonomer composition were studied and correlated with the kinetics of swelling of the grafts in water and ionic solutions. The equilibrium swelling of the grafts depends on the graft composition, as well as the pH and ionic strength of the sorbent. Hosseinzadeh and Mohammadi[25] also reported a maximum in the dependence of the equilibrium swelling of grafted cotton on the graft copolymer composition. However, these substrates are not nearly as inert towards grafting or as nonpolar as ePTFE, and extrapolation of these findings to ePTFE may therefore not be appropriate.

In this manuscript, we examine the preparation and properties of ePTFE membranes grafted with copolymers of AA and IA prepared from aqueous mixtures of AA and IA using the *in situ* $\gamma$-irradiation technique. The grafting yields have been measured at three copolymer compositions and the grafted chains have been characterized using X-ray photoelectron spectroscopy (XPS) and Fourier transform infrared (FTIR) spectroscopy. The compositions of copolymers prepared from mixtures of AA and IA of different composition have been determined in a separate study and this data was fitted to the terminal model for copolymerization to yield information about the graft compositions and sequence distributions. The morphology of the grafted surfaces of the ePTFE has been investigated by scanning electron microscopy (SEM) analysis and the ability of the grafted chains to uptake water examined.

## EXPERIMENTAL

### Materials

AA and IA were purchased from Sigma Aldrich. The AA, 99% pure containing 180–200 ppm monomethyl ether hydroquinone (MEHQ) inhibitor, was purified by vacuum distillation (copolymerization) or passage through a column of MEHQ remover (Sigma-Aldrich product number 311332) (grafting). The IA had a purity of >99%. The ePTFE membrane was obtained from Pall Corporation under the trade name of "Zefluor$^{TM}$ 1.0 $\mu$m", where the 1.0 $\mu$m refers to the pore size in the membrane. 1,4-Dioxane (DO) was obtained from the Merck Chemical Co. and was used as an internal reference in the NMR study. Deuterium oxide ($D_2O$) was purchased from Cambridge Isotope Laboratories and used as the NMR solvent. A water-soluble initiator, Vazo56, was used for the copolymerization study and was obtained from DuPont. It has a half-life of 8.1 h at 62°C. Milli Q water was used as a solvent. Methanol (MeOH) $\geq$ 99.8% was obtained from Merck and dichloromethane from Fisher Scientific. Ammonium iron (II) sulfate hexahydrate 99% (Mohr's salt) was obtained from Sigma-Aldrich. BioWhittaker® phosphate-buffered saline (PBS) was from Lonza.

### Copolymerization

Aqueous solutions of AA and IA (total monomer concentration 3 mol $L^{-1}$) containing Vazo56 initiator (0.008 mol $L^{-1}$) were prepared for the kinetic studies. After preparation, the solutions were transferred into 20 mL glass tubes sealed with a suba seal, and bubbled with nitrogen gas for 20 min to exclude oxygen. The tubes were then placed in a water bath at a temperature of 62 $\pm$ 0.2°C to initiate polymerization. Periodically an aliquot of 200 $\mu$L was sampled from each of the polymerizing mixtures and the sample rapidly quenched to 25°C by adding it to an NMR tube containing 1 mL of $D_2O$ to which a small amount of DO had been added.

The $^1$H NMR measurements (400 MHz Bruker AV NMR) were performed at room temperature using a 45° pulse angle and a recycle delay of 10 s in all cases. This combination of relaxation delay and pulse angle was shown to allow complete relaxation of the protons of both the AA and IA monomers. The intensities of the double bond peaks of the monomers were indexed using the DO reference and the peak areas obtained by integration. The error in measuring the initial monomer feed composition of the monomers was estimated to be less than 1% and for the relative polymerization rates obtained from the NMR spectra to be less than 5%.

The terminal model reactivity ratios for the copolymerization were calculated from the initial rates of polymerization of the two monomers and the corresponding monomer feed compositions using eq. (1) and a computer program reported by Hill and O'Donnell.[26]

$$\frac{dC_A/dt}{dC_I/dt} = \frac{(C_A)(r_{AA}C_A + C_I)}{(C_I)(r_{IA}C_I + C_A)} \quad (1)$$

where $C_A$ is the feed concentration of AA; $C_I$ is the feed concentration for IA; $r_{AA}$ and $r_{IA}$ are the reactivity ratios for AA and IA, respectively.

### Grafting

For the grafting experiments, requisite quantities of AA and IA were added to a test tube containing 4 mL of MilliQ water containing 40 mg of Mohr's salt. The ePTFE samples (weight 7–12 mg, dimension of 10 mm $\times$ 15 mm) were placed into the monomer solution. The test tubes were closed by suba-sealed stoppers and the dissolved oxygen in the solution was removed by bubbling with nitrogen gas for 15 min. The samples were then further sealed using parafilm. The samples were subsequently irradiated at ambient temperature by $^{60}$Co $\gamma$-radiation to a dose of 10 kGy using a Nordian Gamma Cell-220 (dose rate of 1.5 kGy/h). After irradiation, the grafted samples were subjected to washing with hot MeOH to remove unreacted monomer and occluded polymer. The grafted samples were further washed in MilliQ water three times for 1 h and finally left in water overnight. Lastly, samples were dried in a desiccator for 3 days until a constant weight was achieved. Energy-dispersive X-ray microanalysis (EDX) and X-ray photoelectron

spectroscopy (XPS) analysis of the samples detected no Fe(II) ions in the grafts after the washing procedure was complete.

### Characterization

Graft yields were determined from initial and final weights obtained using a Mettler Toledo XS205 balance (0.00 mg accuracy). The average graft yield was calculated from duplicate measurements using eq. (2).

$$\text{Graft Yield } (\%) = \frac{W_f - W_i}{W_i} \times 100\% \quad (2)$$

where $W_f$ is the weight of grafted sample and $W_i$ is the initial weight of the ePTFE sample.

XPS was used to analyze the chemical composition of the surface and was performed on a Kratos Axis Ultra X-ray photoelectron spectrometer using a monochromated Al Kα source (1486.6.6 eV) at 15 kV and 10 mA (150 W) with a vacuum system giving a base pressure of $\sim 10^{-8}$ Torr. Survey scans were carried out at 1200–0 eV with 1.0 eV steps at a pass energy of 160 eV; narrow scans used 0.1 eV steps at a pass energy of 20 eV. The binding energy of the samples was corrected based on the value for the C—F peak of 292.1 eV.[27] CasaXPS software was used to calculate the atomic concentrations and to curve fit the high resolution data. Refinement for peak height was done after all component energies, number of peaks, and peaks widths were fixed initially based on previously published data.[27] The graft extent was determined from the XPS carbon narrow scan using eq. (3) previously described.[28]

$$\text{Graft Extent } (\%) = \frac{C_{\text{All}} - C_{C-F}}{C_{\text{All}}} \times 100\% \quad (3)$$

where $C_{\text{All}}$ is the percent concentration of all carbon bond components present in the sample scan and $C_{C-F}$ is the percent of the carbon-fluorine bonded carbons. The average and standard deviation are reported based on duplicate samples.

Attenuated total reflectance infrared spectra (8 scans, 4 $cm^{-1}$ resolution, wave number range 550–4000 $cm^{-1}$) were recorded using a Perkin Elmer FTIR Spectrum 2000 equipped with a ZnSe crystal (refractive index 2.4381). All FTIR spectra were recorded at ambient temperature.

The X-ray diffraction (XRD) patterns were recorded on a Bruker D8 Advance X-Ray diffractometer with a Cu Kα source ($\lambda = 0.1542$ nm). The scans were performed at a speed of 0.02°/1.2 s, ranging from $2\theta = 10$–70° at 40 kV and 30 mA. Spectra were analyzed using Diffrac$^{\text{plus}}$ Topas software and the percentage crystallinity was calculated from the crystalline and total areas of the diffractogram by using the range $2\theta = 11$–21°.[29]

Water uptake was obtained by immersing untreated and grafted ePTFE membranes in water overnight at 25°C or in PBS solution at 37°C. The samples were removed from the water and filter paper was used to remove any surface water before the sample weight was determined. The equilibrium water uptake, $Q_e$, was calculated using eq. (4).

$$Q_e = \frac{W_s - W_d}{W_{\text{graft}}} \times 100\% \quad (4)$$

where $W_s$ is the weight of the swollen sample, $W_d$ is the dry sample weight, and $W_{\text{graft}}$ is the mass of AA or AA-*co*-IA on the grafted membrane. The average and standard deviation are reported based on at least duplicate samples.

SEM analysis was performed using either a JEOL JSM 6300 or 6610 microscope. All samples were coated with platinum for 5 min until a 15-nm thick layer had formed in order to make the material conductive. SEM analysis was performed using the standard high vacuum mode and the voltage was kept at 5 kV throughout the analysis. The morphology of each sample was imaged at a variety of magnifications.

For tensile measurements, ePTFE samples were cut into a dog-bone shape with a 14 mm gauge length and 2 mm width using cutter ISO-37 type 4. The tensile test was performed using an INSTRON 5543 machine. Young's modulus ($E$) was determined using the slope of the stress–strain curve in the elastic region. Ultimate tensile strength (UTS) (the maximum stress achieved before rupture) and percentage elongation at break ($\varepsilon$) were also obtained from the stress–strain curves. Each sample type was run on a minimum of 5 replicates and the values reported are the mean ± standard deviation.

Contact angle measurements were performed on a custom-built instrument which has been described in detail previously.[30] MilliQ water drops (5 μL) were placed on the surface of the sample using a 50 μL glass flat-tipped syringe and images of the drop captured and analyzed by Scion Image processing software. The advancing angles ($\theta_A$) were measured by successive 5 μL additions of water to a total of 20 μL. The data are reported as the mean ± standard deviation.

## RESULTS AND DISCUSSION

### Copolymerization Reactivity Ratios

A series of mixtures of AA and IA monomers of different compositions were prepared for polymerization at 62°C, as outlined in Table I. A typical $^1$H NMR spectrum of a sample containing a feed mole fraction, $f_{\text{AA}}$, of 0.466 before polymerization is shown in Figure 1. The structures of the two monomers and the assignment of the monomer peaks in Figure 1 are outlined in the inserted scheme. The doublets labeled "a" and "b" in the spectrum arise from the methylene protons of the AA and the quartet labeled "c" arises from the methine proton. The peaks "d" and "e" are the methylene proton peaks from the double bond of IA and peak "f" is the side-chain methylene proton peak. Peak "g" arises from the DO reference in the solution. Most of the peaks are baseline resolved, but the quartet of peaks at 6.1 ppm, labeled "c" in the spectrum, which are characteristic of AA and the peak at 5.8 ppm, labeled "e" which is characteristic of IA were used to monitor the consumption of the two monomers during polymerization. The areas of peak "c," $A_c$, and of peak "e," $A_e$ were used to calculate the concentrations of the two monomers, $C_A$ and $C_I$, throughout the polymerization, the percentage conversion of the monomers and the initial rates of polymerization of each monomer.

A typical series of NMR spectra showing the changing peak intensities with polymerization time is presented in Figure 2, and the evolution of the conversion for the individual monomers is shown in Figure 3 for a copolymerization at a feed mole fraction, $f_{\text{AA}}$, of 0.883. The $^1$H NMR relative peak

**Table I.** Monomer Feed Mole Fractions of the Samples for Copolymerization

| Sample | $f_{AA}$ | $f_{IA}$ |
|---|---|---|
| 1 | 0.399 | 0.601 |
| 2 | 0.466 | 0.534 |
| 3 | 0.592 | 0.408 |
| 4 | 0.658 | 0.342 |
| 5 | 0.789 | 0.211 |
| 6 | 0.883 | 0.117 |

The overall monomer concentration in the mixtures was 3 mol $L^{-1}$.

intensities for each of the monomers shown in Figure 3, which are proportional to the concentrations of the monomers in solution, decrease exponentially with time as expected. The fitted curves are shown in the figure and the rate parameters describing the two curves obtained by exponential regression are $4.17 \pm 0.09 \times 10^{-2}$ $min^{-1}$ for AA and $5.3 \pm 0.3 \times 10^{-2}$ $min^{-1}$ for IA ($R^2 > 0.994$). Similar results were obtained for the other five copolymerization mixtures. As the initial mole fraction of AA in the feed mixture decreases, the rate of the copolymerization also decreases.

The relationship between the initial composition of the copolymer formed during copolymerization, calculated from the rate parameters obtained from the exponential curve fits such as those shown in Figure 3, and the corresponding initial feed composition of the monomers is presented in Figure 4. The reactivity ratios of the two monomers for the terminal model for copolymerization at 62°C were calculated from this data through the use of eq. (1) using a nonlinear regression analysis.[26] The fitted curve shown in Figure 4 provides a good representation of the initial experimental feed and copolymer composition data.

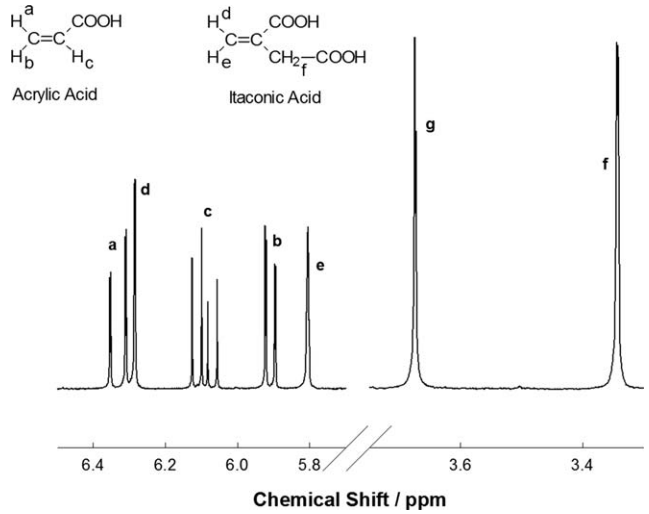


**Figure 1.** $^1$H NMR spectrum of a mixture of the AA and IA ($f_{AA} = 0.466$) monomers obtained during polymerization showing the peak assignments; insert monomer structures with the protons labeled for assignment. Peak "g" is the dioxane reference peak.

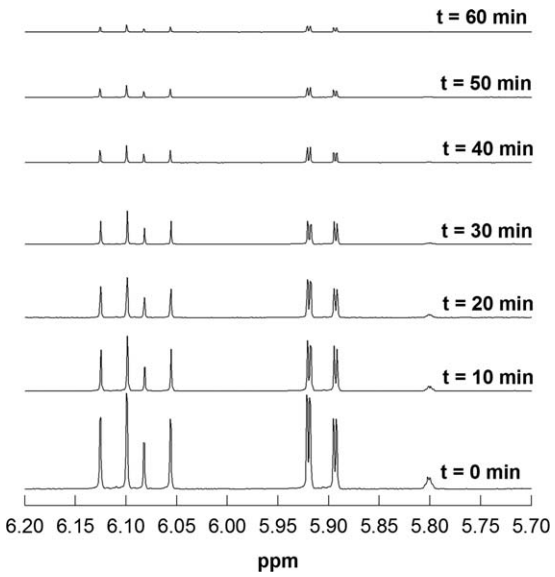


**Figure 2.** Typical $^1$H NMR spectra of a polymerizing mixture of AA and IA at 62°C obtained at various polymerization times. The spectra were indexed using a dioxane reference peak. Double bond peak assignments are shown in Figure 1.

The best values of the reactivity ratios obtained from the curve fit for the terminal model were $r_{AA} = 0.661$ and $r_{IA} = 1.096$, and the corresponding 90% confidence ellipsoid is shown in the Figure 4 insert. The average sequence lengths for each of the monomers were calculated from the reactivity ratios using equations that have been reported previously.[26] For a comonomer mole fraction of $f_{AA} = 0.5$, the average sequence lengths of both the AA and IA monomers predicted from the reactivity ratios is ~2, but for a copolymer mole fraction of 0.9 the average sequence lengths for AA and IA are ~7 and 1, respectively.

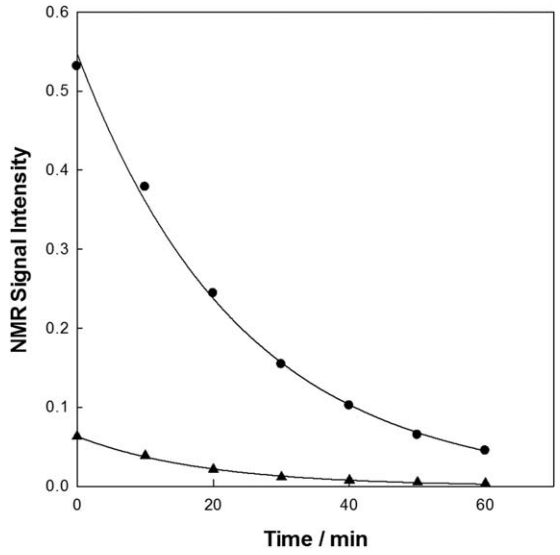


**Figure 3.** $^1$H NMR signal intensity versus time for a polymerizing monomer mixture at 62°C with an initial $f_{AA}$ of 0.883. The signal intensity is proportional to the monomer concentration in the reaction mixture. AA, ●; IA, ▲; the solid lines are exponential regression curve fits to the experimental data.

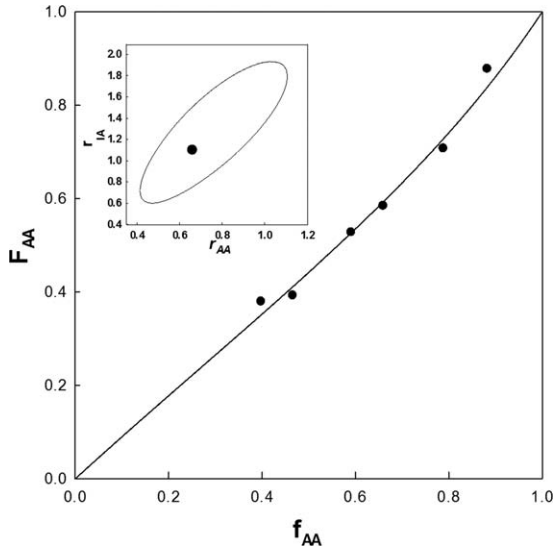


**Figure 4.** Relationship between the AA initial feed, $f_{AA}$, and copolymer, $F_{AA}$, compositions for copolymerization of AA and IA at 62°C, showing the best fit line for the terminal model for copolymerization and the corresponding values of the reactivity ratios and the 90% ellipsoid of confidence (insert).

Thus at $f_{AA} = 0.9$ the IA monomer reduces drastically the average length of the AA sequences compared to that for an AA homopolymer, and they are further reduced at lower values of $f_{AA}$.

### Properties of the Pall Corporation ePTFE

As shown in Figure 5, the "Zeflour™ 1.0 $\mu$m" membrane has a layered structure. One face of the membrane (side 1) has a microporous morphology consisting of both islands and fibrils typical of ePTFE, whereas the other face (side 2) has a porous morphology without any fibrillar structure. Tensile tests showed different properties for the two faces, where one side (side 1) has a higher Young's Modulus than the other side (for side 1 $E = 57 \pm 9$ MPa and for side 2 $E = 28 \pm 3$ MPa). The UTS of side 1 was 35 MPa and $\varepsilon$ was 156%. For this research, only the ePTFE membrane (side 1) was of interest for surface modification and characterization, so side 2 was removed by peeling the two faces apart with forceps. The thickness of ePTFE side 1 after separation was 10 $\mu$m.

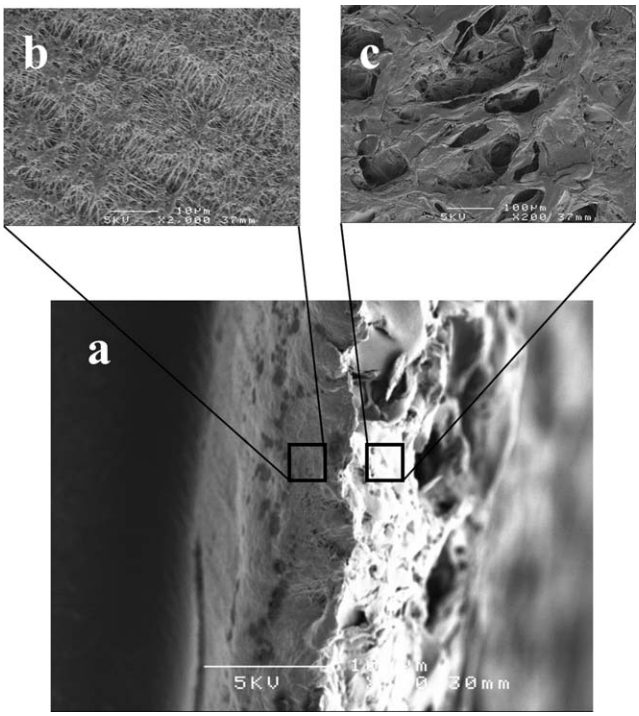


**Figure 5.** SEM image of (a) Pall Corporation ePTFE, (b) side 1, and (c) side 2.

The ePTFE membrane was found by DSC analysis to have two thermal transitions (data not shown), one at 334°C and one at 377°C. The endothermic peak at 334°C is typical of phase melting,[31] while the endotherm at 377°C is a consequence of the PTFE having been expanded, thereby creating a node-fibril structure.[3,31] The percentage crystallinity of the ePTFE membrane was determined to be 43% by including both thermal transitions, and based on a melting enthalpy of 82 J/g for 100% crystallinity.[32] XRD patterns (data not shown) of the ePTFE displayed an intense peak at around 18° attributed to the (100) reflection, which arises from the lateral two-dimensional hexagonal packing of PTFE chains.[29] Considerably, weaker peaks were observed at 32° and 37° corresponding to the 110 and 200 diffractions, respectively. The percentage crystallinity of the ePTFE obtained from the XRD pattern, determined from the integral of the 100 peak and the amorphous halo using the $2\theta$ position which ranged from 11 to 21°,[29] was found to be 59%. This value is significantly higher than that determined using DSC and is attributed to XRD measuring the response not only from the crystalline but also the paracrystalline phases of the polymer while DSC records only the melting of the thermodynamically stable crystalline phase.[7]

### Characterization of Grafted ePTFE

Under radiation exposure, the ePTFE will undergo chain scissions and a loss of fluorinated fragments and carbon centered radicals will be formed in the ePTFE. However, at a dose of 10 kGy, the matrix properties of the ePTFE will not be severely affected.[7] The radicals formed at the ePTFE surface can initiate polymerization of the surrounding monomers, so covalently bonded grafts will be formed at the ePTFE surface. Because the same dose has been used for all of the grafts studied herein, the number of radicals formed at the ePTFE surface will be the same in each case, so the same number of surface graft sites may be expected for all of the samples.

The graft yields were measured by the mass change and the results displayed in Table II. The graft yield for AA grafts increased with increasing monomer concentration, and the results obtained here are in good agreement with our earlier study of AA grafts on "Zeflour™ 0.5 $\mu$m" membranes.[7] The graft yield for IA is much lower than that for AA at a similar monomer concentration. For example, the graft yield for a 0.77 mol $L^{-1}$ IA solution, expressed as moles of monomer per 100 g of ePTFE, is approximately two orders of magnitude smaller than for AA at the same concentration. The lower IA graft yields can be explained by the low reactivity of the bulky

**Table II.** Grafting Conditions and Results for the Monomers onto ePTFE

| Sample | $X_{AA}$ | Monomer concn. (mol $L^{-1}$) | Graft yield (%) | Graft yield (mol/100 g) |
|---|---|---|---|---|
| IA1 | 0.0 | 0.15 | 0.7 | 0.005 |
| IA2 | 0.0 | 0.77 | 0.5 | 0.004 |
| (AA-*co*-IA)1 | 0.40 | 3.0 | 51 ± 1 | 0.48 ± 0.01 |
| (AA-*co*-IA)2 | 0.70 | 3.0 | 48 ± 2 | 0.54 ± 0.02 |
| (AA-*co*-IA)3 | 0.90 | 3.0 | 36 ± 3 | 0.46 ± 0.04 |
| AA1 | 1.0 | 0.28 | 18 ± 4 | 0.25 ± 0.06 |
| AA2 | 1.0 | 1.34 | 35 ± 1 | 0.49 ± 0.01 |

IA chain end radical, which leads to a lower homopolymerization rate for IA compared with AA.[33] Grafting of AA-*co*-IA comonomer mixtures resulted in high graft yields (see Table II), and these only showed relatively small variations with monomer feed composition. This highlights the advantage of incorporating AA in the grafting solution when grafting a bulky monomer (e.g., IA).

An FTIR spectrum of the ePTFE membrane before grafting is given in Figure 6(a). The spectrum displayed the main characteristic asymmetric $CF_2$ stretch at 1207 $cm^{-1}$, the symmetric $CF_2$ stretch at 1152 $cm^{-1}$ as well as minor $CF_2$ wagging (636 $cm^{-1}$) and $CF_2$ deformation (553 $cm^{-1}$) vibrational modes.[34] Additional bands were observed in the FTIR spectrum after radiation induced grafting of the monomers [spectra given in Figure 6(b,c)], most noticeably a broad band at 1716 $cm^{-1}$ which is assigned to the carbonyl band of the grafted carboxylic acid groups. Observation of this band confirms that grafting has occurred for each of the monomer systems studied. In addition, all the grafts displayed a very broad band at 3000–3600 $cm^{-1}$ attributed to a carboxylic acid OH stretching vibration (or to bound water), while C—H stretching and bending vibrations are observed at 2850–2970 $cm^{-1}$ and 1340–1470 $cm^{-1}$, respectively.[35] It was observed that the intensities of these bands increased relative to the CF bands at higher grafting yields.

The surface morphology of the virgin and grafted membranes was examined by SEM. The ePTFE membrane was observed to contain fibrils interconnecting nodal regions in the matrix [see Figure 7(a)]. The fibrils were ~4 $\mu$m long and 0.1 $\mu$m wide. The fibrils connecting the islands are randomly orientated in these membranes. Modification of the ePTFE membrane surface with IA did not cause any visible change in the surface morphology [see Figure 7(b)], but modifications with AA and AA-*co*-IA copolymers resulted in significant, observable morphological alterations to the surface. Typical SEM images for samples AA2 and (AA-*co*-IA)2 are also shown in Figure 7(c,d), respectively. The images reveal that the ePTFE surfaces of these grafted samples are covered by a globular material and that these features dominate, but in some regions it is difficult to assess if the morphology is that of the graft or the underlying substrate.

An XPS survey scan of the ePTFE surface [Figure 8(a)] indicated the presence of carbon and fluorine peaks. These peaks were also observed in all of the grafted samples [Figure 8(b,c)]. In addition to carbon and fluorine peaks, an oxygen peak was observed for the grafted membranes. The intensities of the oxygen peaks were significantly higher for the samples grafted with an AA-*co*-IA copolymer. The untreated membrane showed a single C1s carbon peak while the AA, IA, and AA-*co*-IA copolymer grafted samples showed a carbon doublet peak [Figure 8(b,c) gives examples], again indicating successful grafting.[27]

O1s narrow scans of grafted samples, which are representative of all the grafted samples, are shown in Figure 9(c,e). The spectra can be simulated with just two oxygen peaks, *O*—C═O at 532.2 eV and O—C═*O* at 533.6 eV, as demonstrated in Figure 9. In addition, the O1s scans for the AA grafts were very similar to those reported by Beamson and Briggs for PAA.[27] Thus, the XPS high resolution O1s spectra indicate that —COO is the only significant oxygenated species present in the grafts. The high resolution C1s spectrum of the untreated ePTFE membrane [Figure 9(a)] showed a single carbon peak at 292 eV which represents *C*$F_2$, while the high resolution C1s spectra of the grafted samples displayed a peak at 292 eV as well as an envelope of peaks in the region of 285–290 eV. Curve fitting to the envelope, demonstrated in Figure 9(b,d), showed the presence of four nonfluorinated carbon components in the spectra; *C*OO at 289 eV, *C*—COO at 286 eV, C—C at 285 eV, and a small *C*—O or *CH*—$CF_n$ peak at 287 eV.[27,36,37] The latter peak was always of small intensity and observed to have approximately the same intensity relative to the total area of all the carbon peaks in the C1s spectrum. The areas of each of the nonfluorinated carbon peaks in the C1s spectra were calculated relative to the total area of these peaks, and the fractional areas

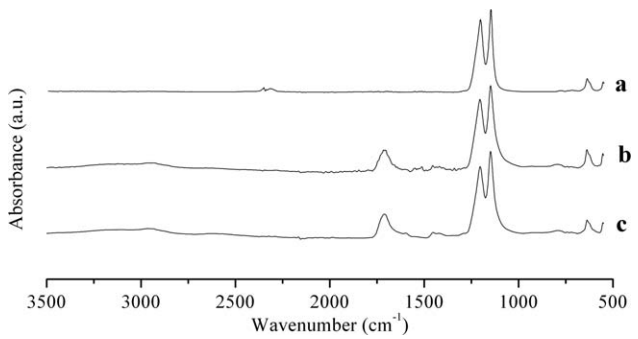


**Figure 6.** FTIR spectra for (a) untreated ePTFE, (b) grafted sample AA2, and (c) grafted sample AA-*co*-IA2.

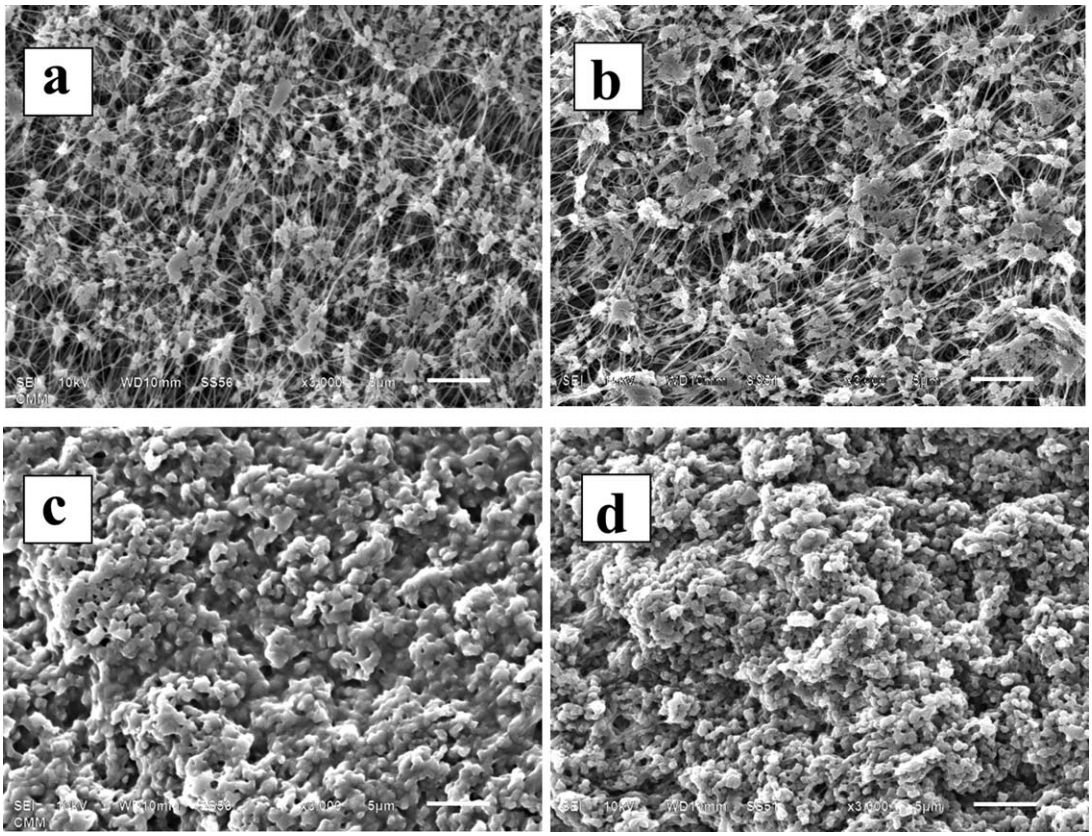


**Figure 7.** SEM images of (a) untreated ePTFE, (b) grafted sample IA2, (c) grafted sample AA2, and (d) grafted sample AA-*co*-IA2. Scale bar in all images is 5 $\mu$m.

for COO are given in Table III. During curve fitting, the fractional intensities for *C*OO and *C*—COO were set to be equivalent based on the chemical structure of the grafted homopolymers and copolymers. However, these fractions are lower than expected for a pure polymer or copolymer graft (e.g., 0.33 for AA and 0.4 for IA). On the other hand, the fractions for *C*—C are correspondingly much higher than those expected for these polymer grafts based on their chemical structures. Although decarboxylation of the polymer graft during radiolysis has previously been suggested,[38] it cannot explain our data based on a G-value of 12 for decarboxylation of PAA on radiolysis in the solid state[39] and a total does of 10 kGy (e.g., less than one carboxyl group per million would undergo decarboxylation). We therefore attribute this observation to adsorption of carbon impurities onto the grafted membranes.

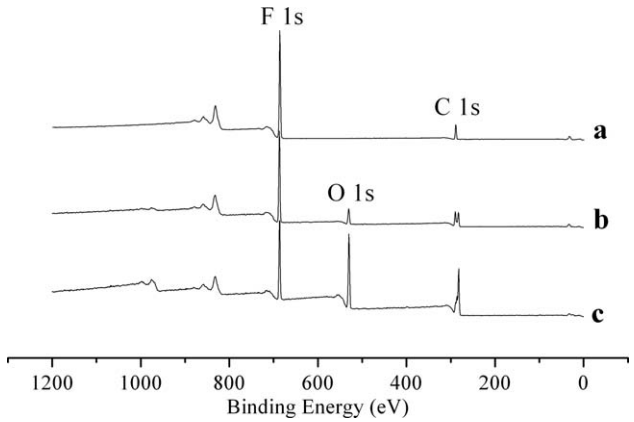


**Figure 8.** XPS survey scans of (a) untreated ePTFE, (b) grafted sample AA2, and (c) grafted sample AA-*co*-IA2.

As mentioned above, the C1s area fractions of the peak at 287 eV (assigned to *C*—O or *C*H—$CF_n$ graft points) are small. The presence of *C*—O could indicate oxidation occurs, but ePTFE irradiated in water in the absence of monomer did not show a peak at 287 eV and the 287 eV peak is only present for grafted samples. A possible explanation for the presence of a *C*—O peak, which would be consistent with both the C1s and O1s narrow scan data, is that the grafts have undergone inter- or intra-molecular esterification during the grafting process. However, such reactions have never been observed previously for irradiated PAA to the best of our knowledge. While a peak at 287 eV observed for PAA thin films deposited on oxidized metal substrates was attributed to a *C*—O peak formed as a result of damage caused by the XPS X-ray irradiation during the analysis,[40] such a reaction during XPS analysis does not appear to occur for bulk PAA[27] or AA grafted ePTFE.[7] We therefore attribute the 287 eV peak to *C*H—$CF_n$ grafting points where the graft copolymers are bonded to fluorinated carbon atoms on the ePTFE surface.[36,37] This assignment is in agreement with this peak being of similar intensity for all the samples and the expected similar number of surface graft sites for all the samples as a result of using a constant radiation dose.

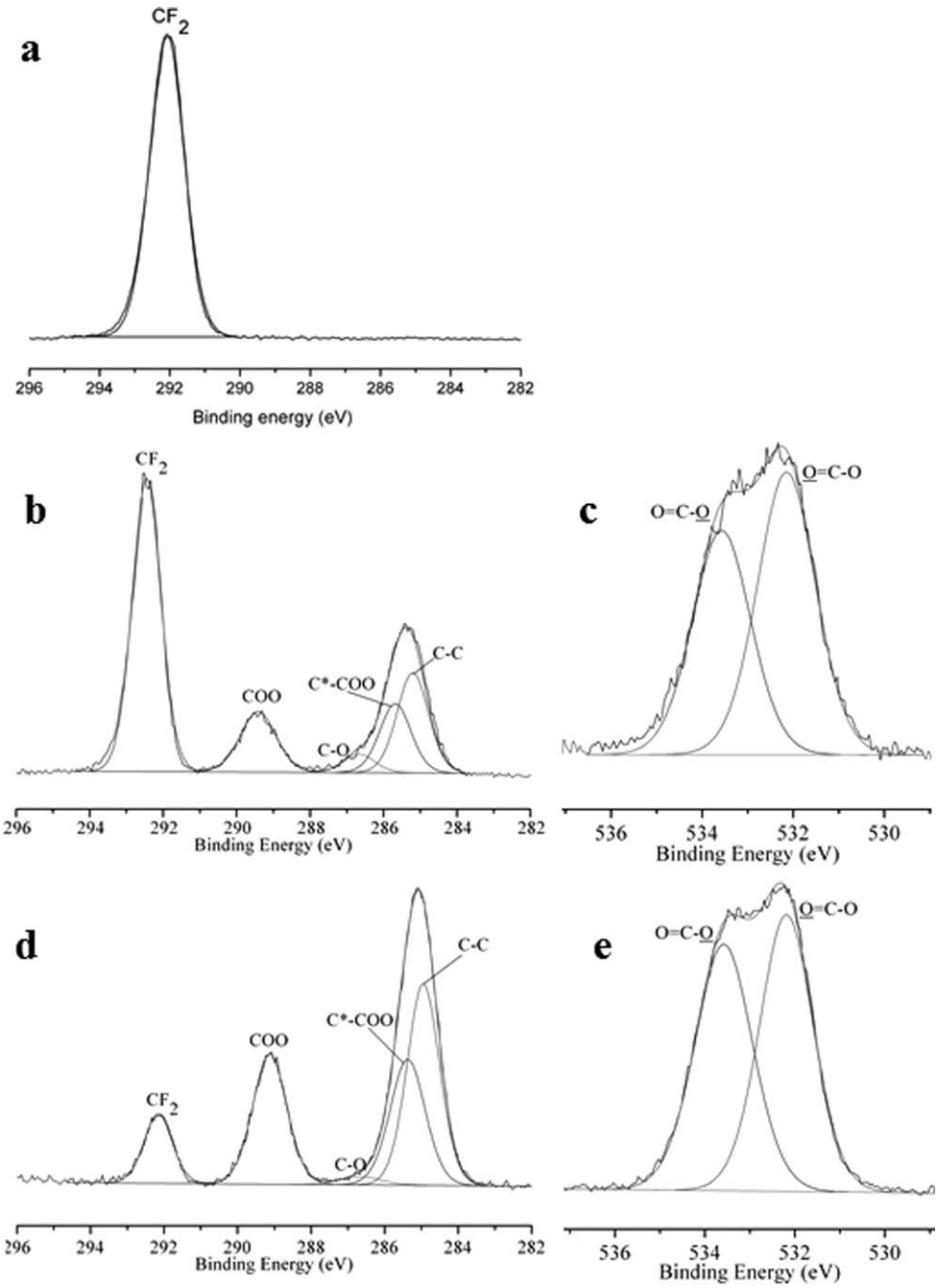


**Figure 9.** XPS narrow scans. (a) C 1s for untreated ePTFE; (b) C 1s for grafted sample AA2; (c) O 1s for sample AA2; (d) C 1s for grafted sample AA-*co*-IA2; (e) O 1s for grafted sample AA-*co*-IA2.

The graft extents were determined from the XPS analysis and compared with the grafting yields. The grafting extent reflects the amount of graft at the surface of the substrate, as distinct from the grafting yield which measures the total amount of graft. For the AA grafts, the graft extent increased with increasing monomer concentration (see Table III), and the results obtained are in good agreement with our earlier study of AA grafts on "Zeflour$^{TM}$ 0.5 $\mu$m" membranes.[7] On the other hand, the graft extent for IA is much lower than that for AA at a similar monomer concentration. However, while the IA graft yield for a 0.77 mol $L^{-1}$ solution, expressed as moles of monomer per 100 g of ePTFE, was approximately two orders of magnitude smaller that for AA at the same concentration, the corresponding grafting extents only differed by a factor of ~2. These results suggest that a higher proportion of the IA graft is located at or near the outer surface of the ePTFE compared with the AA graft, which being formed from a more reactive monomer, extends further into the substrate. Grafting of AA-*co*-IA co-monomer mixtures resulted in high graft extents and graft yields (see Tables II and III), which showed relatively small variations with monomer feed composition.

**Table III.** XPS Results for Grafting of the Monomers on ePTFE

| Sample | $X_{AA}$ | Area fraction COO | Area fraction C—C | Graft extent[a] (%) |
|---|---|---|---|---|
| IA1 | 0.0 | 0.18 | 0.45 | 14 |
| IA2 | 0.0 | 0.20 | 0.38 | 18 |
| (AA-*co*-IA)1 | 0.4 | 0.28 | 0.40 | 66 ± 45 |
| (AA-*co*-IA)2 | 0.7 | 0.28 | 0.39 | 84 ± 8 |
| (AA-*co*-IA)3 | 0.9 | 0.27 | 0.43 | 71 ± 18 |
| AA1 | 1.0 | 0.29 | 0.29 | 31 ± 1 |
| AA2 | 1.0 | 0.27 | 0.43 | 48 ± 3 |

[a] Analyses at different areas on the surface of the samples yielded similar results in each case, but the reproducibility between duplicate samples was low for AA mole fractions of 0.4 and 0.9.

**Table IV.** Equilibrium Water Uptake by the Grafted Polymers and the Average Number of Water Molecules per Carboxyl Group at 25°C

| Sample | $X_{AA}$ | Water uptake (wt %) | Average number of water molecules per COOH |
|---|---|---|---|
| (AA-*co*-IA)1 | 0.4 | 330 ± 200 | 13 ± 8 |
| (AA-*co*-IA)2 | 0.7 | 630 ± 20 | 24 ± 1 |
| (AA-*co*-IA)3 | 0.9 | 440 ± 100 | 16 ± 4 |
| AA1 | 1.0 | 790 ± 30 | 32 ± 1 |
| AA2 | 1.0 | 660 ± 60 | 26 ± 2 |

### Properties of Grafted ePTFE

PTFE films have been characterized as being highly hydrophobic with a water contact angle in air at room temperature of 126°,[41] while that for ePTFE was measured in this work to be 115 ± 6°. In order for ePTFE to be used as a tissue space filler in facial reconstruction where the implant interfaces with bone, its hydrophobic surface is modified and a range of methods have been evaluated as detailed in our recent review.[2] It is desirable to create a surface that more closely mirrors the properties of natural tissue including wettability, swelling of the surface layer, and presentation of suitable functional groups in order to allow better integration of the substrate with facial bone. Building on the work on glass ionomers used for dental applications,[14] this study thus evaluates the potential benefit of forming graft copolymers using monomer mixtures of AA and IA. The AA surface modified ePTFE membranes of this study were found to be much less hydrophobic than ePTFE, with a contact angle of 88 ± 10° for sample AA1 which is larger than that reported for PAA of 50°.[42] Water contact angles in air for PTFE grafted with AA have been reported by other workers,[14] but the fibrillar surfaces of ePTFE have a very different topography to that of PTFE films and sheets. The contact angles obtained for the AA grafts onto ePTFE will be subject to the porous and rough nature of the ePTFE substrate surface. Water contact angles could not be obtained for the AA2 or the AA-*co*-IA grafted membranes because the water droplets were very rapidly absorbed by these materials. Thus, water contact angle measurements could not be used to discriminate between the samples that had graft extents of 48% or more (graft extent values listed in Table III).

While the chemical composition in terms of the presence of carboxylate groups can be evaluated from FTIR and XPS, the polymer topology as well as, in the case of the co-monomers, the composition and sequence distributions of the monomers cannot be attained from this data but can instead be extrapolated from polymers formed in solution. For the grafting of ePTFE with the co-monomers at three different AA mole fractions ($X_{AA}$ of 0.9, 0.7, and 0.4), the average AA sequence lengths of these grafted copolymers can be estimated from the reactivity ratios for the copolymerizations in water, assuming that the reactivity ratios are independent of temperature.[26] Thus, they can be described as having AA sequence lengths of ~7, 2.5, and 1.4 units for $X_{AA} = 0.9$, 0.7, and 0.4, respectively. The grafts in all the graft-copolymers will be subjected to the irradiation, and they will be liable to undergo hydrogen abstraction by hydroxyl radicals formed in the water.[43,44] All of the hydrogen atoms in the graft will be amenable to abstraction. At a dose of 10 kGy, the overall extent of direct damage to the grafted polymer chains (e.g., decarboxylation via direct energy absorption) will be very small based upon radiolysis studies of PAA, for example.[39] The radicals formed on the grafts by hydrogen abstraction can undergo inter- and intra-chain cross linking or disproportionation reactions, the nature of which are determined by the structure of the radicals formed.[43] Depending on the relative proportions of these reaction, the grafted chains may thus form a cross-linked hydrogel network. From previous work, it has been shown that irradiation of PAA solutions (concentration 1.4 mol $L^{-1}$ in AA) at room temperature have gel doses of 3.8 kGy at pH = 2.3 and 27.6 kGy at pH = 2.8, but at high pH no gel is formed.[44] In our study, we evaluated if cross-linked gels formed on irradiation of aqueous solutions of the AA and the co-monomers to a dose of 10 kGy, conditions similar to those used for grafting but without Mohr salt present. It was found that on radiation of an aqueous solution of AA at a concentration of 1.34 mol $L^{-1}$ or an AA/IA mixture with $X_{AA} = 0.9$ at a concentration of 3 mol $L^{-1}$ cross-linked gels were formed. In contrast, on irradiation of 3 mol $L^{-1}$ aqueous solutions of AA/IA mixtures with $X_{AA} = 0.7$ and $X_{AA} = 0.4$ or an AA solution at 0.28 mol $L^{-1}$, no gel was formed, but a water-soluble copolymer was produced. In summary, we can extrapolate that for samples AA1, (AA-*co*-IA)1, and (AA-*co*-IA)2, the grafts will be linear or branched polymers while for samples AA2 and (AA-*co*-IA)3 the grafts can be expected to be a network gel. Furthermore, for sample (AA-*co*-IA)3, the grafts has relatively long AA sequence (of 7 units) while for samples (AA-*co*-IA)1 and (AA-*co*-IA)2 the sequence length in the grafts is much shorter (2.5 and 1.4 units).

Equilibrium water uptakes, $Q_e$, for cross-linked PAA hydrogels in water have been reported to be very large and are dependent on the degree of cross linking, the pH, ionic strength, and the temperature,[45–47] with reported values ranging to more than 1000% at ambient temperature. Swelling measurements in water (see data in Table IV) were carried out on the AA1 and AA2 grafted samples at 25°C and yielded values of $Q_e$ of 790 ± 30%

and 660 ± 60% (mass of water over mass of graft), respectively. However, it should be borne in mind that these equilibrium swelling measurements are subject to significant error because of the relatively small masses of the grafts and the correspondingly small water uptakes. In addition, it has long been recognized that it is very difficult to dry PAA completely without forming anhydrides,[48] so the values of $Q_e$ reported herein (or indeed values reported by other workers) could also be subject to systematic errors. Tanchak et al.[49] have reported that PAA films on hydrophobic silicon surfaces are not swollen homogeneously in water, and that the water concentration is depleted near the PAA/Si interface. If the water concentration in the AA grafts on ePTFE were similarly depleted near the ePTFE-graft interfaces, the number of water molecules per carboxyl group at equilibrium would be less than that observed for a corresponding hydrogel and would increase with the average thickness of the grafted layer. The lower water uptake for AA2 compared with AA1 could result from the expected higher crosslink density of the graft AA2, as this graft will be in the form of a network gel. We have previously reported values of 370% and 270% for the equilibrium swelling of AA grafts on "Zeflour™ 0.5 $\mu$m" ePTFE membranes prepared under similar conditions to AA1 and AA2.[7] The reason for the higher values of $Q_e$ obtained for the "Zeflour™ 1.0 $\mu$m" ePTFE membrane used in the current study is not known unequivocally, but it is believed to be associated with the larger pore size of the substrate (1.0 $\mu$m cf. 0.5 $\mu$m).

The equilibrium water uptake and the average number of water molecules per carboxyl group for the grafts at 25°C, calculated from the graft composition obtained using the AA and IA reactivity ratios, are presented in Table IV. In addition, to model physiological conditions, swelling measurements for the copolymer graft with $X_{AA} = 0.7$ were made in PBS (pH 7.4) at 37°C. The result obtained was $Q_e = 780 \pm 90\%$ (~39 water molecules per carboxyl group) compared with a value of 630% for this copolymer graft in water at 25°C. It is known that $Q_e$ increases for AA hydrogels with an increase in the temperature or the pH.[50] The AA-*co*-IA graft demonstrates this type of behavior.

The equilibrium water uptake values for the AA-*co*-IA grafts were found to be significantly smaller than those obtained for the AA grafted ePTFE. There is some discrepancy in the literature regarding the relative swelling of the equivalent hydrogel systems with a P(AA-*co*-IA) copolymer hydrogel with $X_{AA} = 0.9$ reported by Katime and Rodriguez to swell to a greater extent in water at 25°C than a chemically cross linked PAA hydrogel.[20] The number of water molecules per carboxylic acid group calculated from these data ranged from ~30 for a pure AA hydrogel to ~70 for a hydrogel containing a mole fraction AA of 0.88. On the other hand, Pulat and Eski[19] have shown that $Q_e$ values of cross linked P(AA-*co*-IA) hydrogels are very strongly dependent on pH, and that while at pH = 2 a hydrogel with $X_{AA} = 0.83$ swelled to a greater extent than a pure PAA hydrogel, the order was reversed at pH = 4, with the crossover at about pH = 3. Furthermore, Pulat and Eski[19] have reported the equilibrium swelling of a series of P(AA-*co*-IA) hydrogels swollen in Britton-Robinson solution (pH 7.4) at 37°C and found that the copolymer hydrogels, which ranged in AA mole fraction from 0.66 to 1.00, swelled to a much smaller extent (fewer water molecules per hydroxyl group) than an PAA hydrogel prepared with the same cross linker concentration and this result correlates with our findings (see Table IV). The number of water molecules per carboxyl group for the samples given in Table IV are, however, smaller than those calculated from Katime and Rodriguez's data.[20] Thus, in this respect, the copolymer grafts on ePTFE behave somewhat differently from the corresponding chemically crosslinked bulk hydrogels, presumably because of the presence of the hydrophobic ePTFE substrate constraining swelling of the grafted polymer, particularly if the graft is present within the pores of the substrate. This agrees with the swelling of PAA films on hydrophobic silicon substrates[49] described above.

In our grafted membranes, not only will the mole fraction affect the swelling but also the polymer topology. The copolymer graft for (AA-*co*-IA)3, which contains the highest mole fraction of AA (0.9), will be in the form of a network gel, while the other two copolymer grafts will not form networks. Therefore, $Q_e$ and the average number of water molecules per carboxyl group for (AA-*co*-IA)3 were smaller than the corresponding value for (AA-*co*-IA)2 which has a higher IA mole fraction (0.3). However, the (AA-*co*-IA)1 graft, which contains an even higher mole fraction of IA than (AA-*co*-IA)2, has a lower $Q_e$ than (AA-*co*-IA)2 and a lower average number of water molecules per carboxyl group. This is believed to reflect the lower solubility of IA than AA in water. Hosseinzadeh and Mohammadi[25] have also reported that the $Q_e$ values for chemically crosslinked AA-*co*-IA grafts onto cotton passed through a maximum at a copolymer composition of $X_{AA} = 0.93$, the difference in mole fraction for the cross-over point likely related to cotton being a much more hydrophilic substrate than ePTFE. It is thus clear that extrapolation of findings from grafting to other substrates to ePTFE is not appropriate as the swelling behavior of the grafts are dependent on the underlying substrate.

## CONCLUSIONS

This study has demonstrated the feasibility of grafting a mixture of AA and IA onto ePTFE. The resulting membranes have been shown to be covered by the grafted polymer, to have significantly reduced hydrophobicity, and characterized by high water uptakes. While XPS and FTIR were able to demonstrate the overall chemical changes to the membranes, extrapolation from data obtained from polymers formed in solution was required to evaluate the polymer topology and AA sequence length of the graft copolymers. It was found that the ability of the grafted membranes to swell in water was affected by these properties of the graft copolymers and a complex dependence on polymer chemistry and topology was evident. Furthermore, it was found that the highly hydrophobic nature of the underlying ePTFE membrane affected the ability of the graft copolymers to swell in water with reduced water uptake compared with previously published work on both hydrogel systems and graft copolymers formed on the hydrophilic substrate cellulose.

## ACKNOWLEDGMENTS

The authors thank Dr. Barry Wood for obtaining the XPS data and Dr. Kevin Jack and Ms. Anya Yago for their assistance in the XRD diffraction analysis. Dr. Tri Le is acknowledged for assistance with the NMR studies, Dr. Grant Edwards for assistance with tensile testing, and Dr. Chandhi Goonasekera for providing data for hydrogel synthesis. This work was carried out in part in the Centre for Microscopy and Microanalysis, University of Queensland node of Australian Microscopy and Microanalysis Research Facility (AMMRF). Author Norsyahidah Mohd Hidzir acknowledges the Universiti Kebangsaan Malaysia for a PhD scholarship.

## REFERENCES

1. He, W.; Benson, R. In Handbook of Polymer Applications in Medicine and Medical Devices; Modjarred, K., Ebnesajjad, S., Eds.; Elsevier Science: Oxford, **2014**; Chapter *4*, pp 55–76.
2. Cassady, A. I.; Hidzir, N. M.; Grøndahl, L. *J. Appl. Polym. Sci.* **2014**, *131*, 40533.
3. Wikol, M.; Hartmann, B.; Brendle, J.; Crane, M.; Beuscher, U.; Brake, J.; Shickel, T. In Filtration and Purification in Biopharmaceutical Industry, 2nd ed.; Jornitz, M. W., Meltzer, T. H., Eds.; CRC Press: Boca Raton, Florida, USA, **2008**; Vol. *174*, pp 619–640.
4. Chandler-Temple, A.; Kingshott, P.; Wentrup-Byrne, E.; Cassady, A. I.; Grøndahl, L. *J. Biomed. Mater. Res. Part A* **2013**, 101A, 1047.
5. Yamada, K.; Iizawa, Y.; Yamada, J.; Hirata, M. *J. Appl. Polym. Sci.* **2006**, *102*, 4886.
6. Hegazy, E. A.; Ishigaki, I.; Okamoto, J. *J. Appl. Polym. Sci.* **1981**, *26*, 3117.
7. Hidzir, N. M.; Hill, D. J. T.; Martin, D.; Grøndahl, L. *Polymer* **2012**, *53*, 6063.
8. Njatawidjaja, E.; Kodama, M.; Matsuzaki, K.; Yasuda, K.; Matsuda, T. *Plasma Process Polym.* **2006**, *3*, 338.
9. Gao, J.; Yu, J.; Ma, Y. *Surf. Interface Anal.* **2012**, *44*, 578.
10. Hidzir, N. M.; Hill, D. J. T.; Taran, E.; Martin, D.; Grøndahl, L. *Polymer* **2013**, *54*, 6536.
11. Matsuda, K.; Kawahara, Y.; Shimada, S.; Kashiwada, A.; Yamada, K.; Hitara, M. *J. Photopolym. Sci. Technol.* **2006**, *19*, 225.
12. Chen-Yang, Y. W.; Liao, J. D.; Kau, J. Y.; Huang, J.; Chang, W. T.; Chen, C. W. *Macromolecules* **2000**, *33*, 5638.
13. Akinay, E.; Tincer, T. *J. Appl. Polym. Sci.* **2001**, *79*, 816.
14. Nicholson, J. W.; Croll, T. P. *Quintessence Int.* **1997**, *28*, 705.
15. Culbertson, B. M. *J. Dent.* **2006**, *34*, 556.
16. Culbertson, B. M.; Xie, D.; Johnston, W. M. In Specialty Monomers and Polymers; Havelka K. O., McCormick, C. L., Eds.; ACS Symposium Series 755; **2000**; pp 222–232.
17. Kobayashi, K.; Okamoto, M.; Kawamura, F.; Fukuda, T.; Inden, Y.; Yamamoto, J. *Ger. Pat. DE.* 3,022,924, **1981**.
18. Walinsky, S. W. Eur. Pat. Appl. EP0079165 A3, **1983**.
19. Pulat, M.; Eski, H. *J. Appl. Polym. Sci.* **2006**, *102*, 5994.
20. Katime, I.; Rodriguez, E. *J. Macromol. Sci. Part A: Pure Appl. Chem.* **2001**, *A38*, 543.
21. Huang, Y.; Schricker, S. R.; Culbertson, B. M.; Oleski, S. V. *J. Macromol. Sci. Part A: Pure Appl. Chem.* **2002**, *A39*, 27.
22. Wang, C.; Chen, J.-R. *Appl. Surf. Sci.* **2007**, *253*, 4599.
23. Sadeghi, M.; Yarahmad, M. *Orient. J. Chem.* **2011**, *27*, 453.
24. Sadeghi, M.; Ghasemi, N. *Indian J. Sci. Technol.* **2012**, *5*, 1879.
25. Hosseinzadeh, H.; Mohammadi, S. *Curr. Chem. Lett.* **2013**, *2*, 109.
26. Hill, D. J. T.; O'Donnell, J. H. *Makromol. Chem. Macromol. Symp.* **1987**, *10/11*, 375.
27. Beamson, G.; Briggs, D. The Scienta ESCA300 Database; Wiley: New York, **1992**.
28. Chandler-Temple, A.; Wentrup-Byrne, E.; Whittaker, A. K.; Grøndahl, L. *J. Appl. Polym. Sci.* **2010**, *117*, 3331.
29. Lei, C.; Wang, X.; Fang, Q.; Gao, Y.; Tu, D.; Du, Q. *Eur. Polym. J.* **2007**, *43*, 4523.
30. Chandler-Temple, A. F.; Wentrup-Byrne, E.; Griesser, H. J.; Jasieniak, M.; Whittaker, A. K.; Grøndahl, L. *Langmuir* **2010**, *26*, 15409.
31. Lutz, D. I.; Clough, N. E. U.S. Pat. Appl. US 20060047311 A1, **2006**.
32. Sperati, C. A. In Polymer Handbook; Brandrup, J., Immergut, E. H., Eds.; Wiley-Interscience: New York, **1989**.
33. Grespos, E.; Hill, D. J. T.; O'Donnell, J. H.; O'Sullivan, P. W.; Young, T. L. *Makromol. Chem. Rapid Commun.* **1984**, *5*, 489.
34. Liang, C. Y.; Krimm, S. *Chem. Phys.* **1956**, *25*, 563.
35. Lin-Vien, D.; Colthup, N. B.; Fateley, W.; Grasselli, J. The Handbook of Infrared and Raman Characteristic Frequencies of Organic Molecules; Academic Press Limited: London, **1991**.
36. Shulze, M.; Bolwin, K.; Gulzow, E.; Schnurnberger, W. *J. Anal. Chem.* **1995**, *353*, 778.
37. Clochard, M.; Begue, J.; Lafon, A.; Caldemaison, D.; Bittencourt, C.; Pirreaux, J.-J.; Betz, N. *Polymer* **2004**, *45*, 8683.
38. Alexander, M. R.; Payan, S.; Duc, T. M. *Surf. Interface Anal.* **1998**, *26*, 961.
39. Campbell, K. T.; Hill, D. J. T.; O'Donnell, J. H.; Pomery, P. J.; Winzor, C. L. In The Effects of Radiation on High-Technology Polymers; Comstock, M. J., Ed.; ACS Symposium Series 381; **1989**; pp 80–94.
40. Leadley, S. R.; Watts, J. F. *J. Electron. Spectrosc. Relat. Phenom.* **1997**, *85*, 107.
41. Sun, H.-X.; Zhang, L.; Chai, H.; Chen, H.-L. *Desalination* **2006**, *192*, 271.
42. Ikada, Y. *Biomaterials* **1994**, *15*, 725.
43. Rosiak, J. M.; Janik, I.; Kadlubowski, S.; Kozicki, M.; Kujawa, P.; Stasica, P.; Ulanski, P. Radiation Synthesis and

Modification of Polymers for Biomedical Applications; IAEA-TECDOC-1324: Vienna, **2002**; pp 5–47.

44. Rosiak, J. M.; Ulanski, P.; Pajewski, L. A.; Yoshii, F.; Makuuchi, K. *Radiat. Phys. Chem.* **1995**, *46*, 161.
45. Illescas, J.; Burillo, G. *Macromol. Mater. Eng.* **2009**, *294*, 414.
46. El-Din, H. M. N.; Hegazy, E. A.; Ibraheim, D. M. *Polym. Compos.* **2009**, *30*, 569.
47. El-Din, H. M. N.; Taleb, M. F. A.; El-Naggar, A. W. M. *Nucl. Instrum. Methods Phys. Res. Sect. B* **2008**, *266*, 2607.
48. Marvel, C. S.; Shepherd, T. H. *J. Org. Chem.* **1959**, *24*, 599.
49. Tanchak, O. M.; Yager, K. G.; Fritzsche, H.; Harroun, T.; Katsaras, J.; Barrett, C. J. *Langmuir* **2006**, *22*, 5137.
50. Jabbari, E.; Nozari, S. *Eur. Polym. J.* **2000**, *36*, 2685.